

A Study on the Control Method of Customer Voltage Variation in Distribution System with PV Systems

Byung-ki Kim*, Sung-sik Choi*, Yong-peel Wang**, Eung-sang Kim***
and Dae-seok Rho†

Abstract – This paper deals with the modified modeling of PV system based on the PSCAD/EMTDC and optimal control method of customer voltages in real distribution system interconnected with the photovoltaic (PV) systems. In order to analyze voltage variation characteristics, the specific modeling of PV system which contains the theory of d-q transformation, current-control algorithm and sinusoidal PWM method is being required. However, the conventional modeling of PV system can only perform the modeling of small-scale active power of less than 60 [kW]. Therefore, this paper presents a modified modeling that can perform the large-scale active power of more than 1 [MW]. And also, this paper proposes the optimal operation method of step voltage regulator (SVR) in order to solve the voltage variation problem when the PV systems are interconnected with the distribution feeders. From the simulation results, it is confirmed that this paper is effective tool for voltage analysis in distribution system with PV systems.

Keywords: PV system, Distribution system, PSCAD/EMTDC, d-q transformation, Current-control algorithm, Step voltage regulator, Voltage regulation

1. Introduction

As power systems have been deregulated and decentralized according to the technology development of small-scale distributed generators, PV systems have been actively interconnected and operated in distribution systems. Therefore, many power quality problems such as voltage variations, flicker and harmonic may be occurred, when PV systems are interconnected in distribution system [1-6]. In order to analyze power quality problems like voltage variation characteristics, a specific modeling of PV system considering the theory of d-q transformation, current-control algorithm and sinusoidal PWM method is being required. However, the conventional modeling method of PV system can only deal with the modeling of small-scale active power of less than 60[kW] [7-8]. Therefore, this paper presents a modified modeling that can perform the large-scale active power of more than 1[MW]. In additions, this paper proposes the optimal operation method of the step voltage regulator(SVR) which is located at primary feeder for line voltage control, in order to overcome the voltage variation problem when PV systems are interconnected in distribution system. The case study results show that this paper is effective tool

for voltage analysis and regulation in real distribution system interconnected with PV systems.

2. Modeling for real distribution system

2.1 Distribution system modeling

A single line diagram of real distribution system as depicted in Fig. 1 is usually being used in power utilities, in order to analyze voltage characteristics of low voltage customers. To simplify the complex diagram, this paper divides 6 sections by major points such as circuit breakers, cable size, cable length and branch configurations. And it is assumed that the PV system is located at the end section of real distribution system.

Therefore, the simplified diagram as shown in Fig. 2 can be obtained from the real distribution system.

In order to perform the load modeling of single line diagram, the real values of each section can be obtained from the relationship between estimation value and measured value as follows.

$$I_{(n)} = i_{(n)} \times \frac{I_{SS}}{i_{SUM}} \quad (1)$$

Where, $I_{(n)}$ and $i_{(n)}$ are the real and estimated currents of n section, $I_{(SS)}$ is the measured (real) total current of the main transformer, and $i_{(SUM)}$ is the estimated total current of main transformer.

† Corresponding Author: Dept. of Electrical Engineering, Korea University of Technology, Korea. (dsrho@kut.ac.kr)

* Dept. of Electrical Engineering, Korea University of Technology, Korea. (bkwin@kut.ac.kr)

** Electrical Industry Research Institute of Korea. (ypwang@erik.re.kr)

*** Korea Electric Research Institute, Korea. (eskim@keri.re.kr)

Received: February 14, 2014; Accepted: December 22, 2014

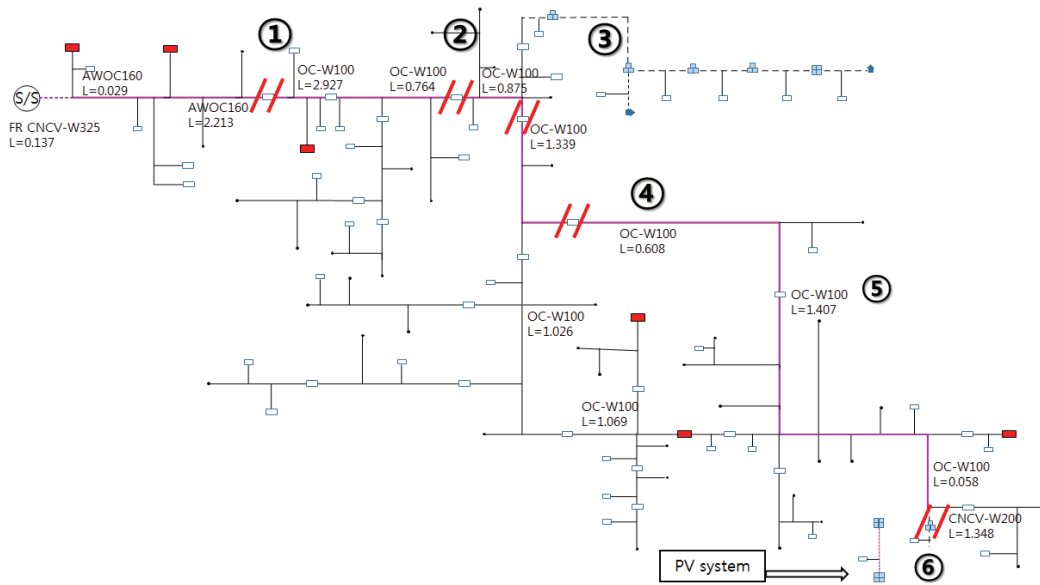


Fig. 1. Single line diagram of distribution system with PV system

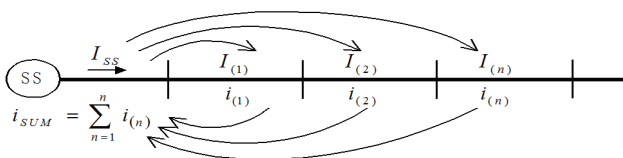


Fig. 2. Simplified diagram of distribution system

2.2 Concept of SVR operation method

This paper adapts a SVR which is installed at primary feeder to compensate the voltage variations. Fig. 3 is the configuration of LDC method of SVR. The decision problem of optimal sending voltages is to find the optimal setting values (V_{ce} , Z_{eq}) of LDC method in order to deliver suitable voltages to as many customers as possible as shown in reference [4]. It firstly determines the ideal optimal sending voltages which can be expressed by the optimal compensation rates of SVR, and then obtains optimal setting values by statistical analysis according to the relationship between ideal optimal sending voltages and total load currents.

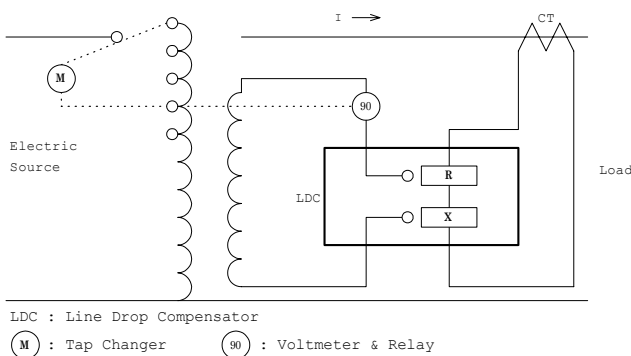


Fig. 3. Concepts for LDC methods

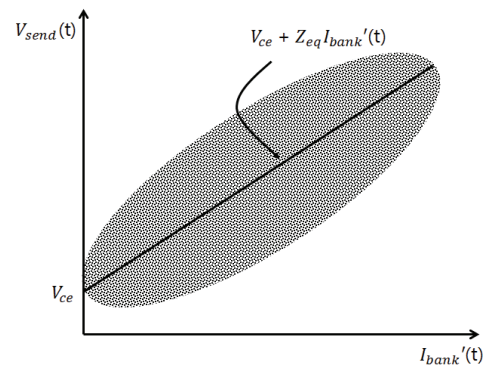


Fig. 4. Distribution characteristics of optimal sending voltages of M.tr

Optimal sending voltages have a general relationship with LDC setting values as shown in Eq. (2). Therefore, the optimal setting values can be calculated by solving the equation for V_{ce} and Z_{eq} .

$$V_{send} = V_{ce} + Z_{eq} \times I_{bank} \quad (2)$$

where, V_{send} is optimal sending voltage, V_{ce} is load center voltage, Z_{eq} is equivalent impedance, and I_{bank} is total load currents of main transformer.

Solving the equation for V_{ce} and Z_{eq} in Eq. (2) cannot provide a linear function and has wide distribution characteristic as depicted in Fig. 4. Therefore, the solution of optimal LDC setting values is equivalent to finding coefficients of the first order equation of Eq. (2). It is desirable to minimize the differences between optimal sending voltages and the first order equation. The Least Square method is now introduced in order to find optimal LDC setting values. The squared summation of differences is formulated as:

$$\text{Min } q = \sum_{t=1}^T \{V_{send}(t) - V_{ce} - Z_{eq} \times I_{bank}\}^2 \quad (3)$$

where, q is error function and T is total number of time interval.

By minimizing q in Eq. (3), V_{ce} and Z_{eq} can be obtained as :

$$Z_{eq} = \frac{\left\{ \sum_{t=1}^T I_{bank}'(t) * \sum_{t=1}^T V_{send}(t) - T \sum_{t=1}^T I_{bank}'(t) * V_{send}(t) \right\}}{\left\{ \left(\sum_{t=1}^T I_{bank}'(t) \right)^2 - T \sum_{t=1}^T \left(I_{bank}'(t) \right)^2 \right\}} \quad (4)$$

$$V_{ce} = \frac{\left\{ \sum_{t=1}^T I_{bank}'(t) * V_{send}(t) - Z_{eq} \sum_{t=1}^T \left(I_{bank}'(t) \right)^2 \right\}}{\sum_{t=1}^T I_{bank}'(t)} \quad (5)$$

In additions, SVR with the $\pm 10\%$ voltage compensation ability are generally composed of 17 tap positions having the each interval of 1.25%. By considering the relationship between sending voltage and nominal voltage (13,200V, phase voltage), each tap position can be formulated by Eq. (6).

$$T_p = (V_{send} - V_n) / (T_{int} \times V_n) + T_s \quad (6)$$

where, T_p is tap position, V_{send} is sending voltage, V_n is nominal voltage, T_s is reference tap number, and T_{int} is tap interval (1.25%).

3. PV Modeling Based on the PSCAD/EMTDC

3.1 Concept for current control algorithm

The configuration of the control block diagram in PV systems can be generally expressed as depicted in Fig. 5. This paper categorizes 4 steps to simplify the diagram.

[Step 1] The 3-phase voltage and current of distribution

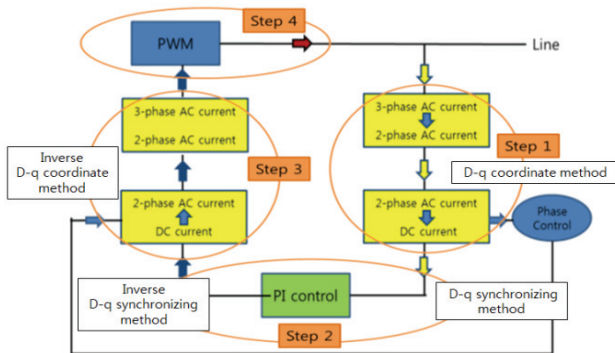


Fig. 5. Control block diagram of PV system

system are converted into 2-phase voltage and current of the d-q stationary coordinate by using the d-q transformation method. And then 2-phase voltage and current are transformed into DC voltage and current of the d-q synchronizing coordinate to easily control the desired voltage and current.

[Step 2] To obtain the reference value for desired current, the DC current of [Step 1] is controlled by the PI controller as shown in Eq. (7) and Eq. (8). In this process, the decoupling control of active and reactive power of PV system can be performed separately.

$$V_{qe-fb} = (I_{qref} - I_{qe}) \cdot \left(k_p + \frac{k_i}{s} \right) + I_{de} \cdot \omega L + V_m \quad (7)$$

$$V_{de-fb} = (I_{dref} - I_{de}) \cdot \left(k_p + \frac{k_i}{s} \right) + I_{qe} \cdot \omega L \quad (8)$$

where, V_{qe-fb} is voltage of q axis, V_{de-fb} is voltage of d axis, $k_p + \frac{k_i}{s}$ is PI controller I_{qref} is the reference current, I_{qe} and I_{de} are output current of inverter which is converted to q axis and d axis, ωL is internal reactance for feed-forward Compensation, and V_m is instantaneous voltage of distribution system.

[Step 3] The DC voltage compensated by PI controller of [Step 2] is reversely converted into 3-phase AC current and voltage by inverse d-q transformation method, where PLL (Phase Locked Loop) circuit is used to synchronize the voltage of distribution system.

[Step 4] In order to control the 6 PWM signals, the converted 3-phase AC voltage of [Step 3] is compared with the comparator with the triangle waveform. The IGBT (Insulated Gate Bipolar Transistor) devices are driven by the 6 PWM signals, and then the DC voltage and current of PV system can be converted into the AC voltage and current of distribution system.

Furthermore, instantaneous active power (P) and reactive power (Q) in balanced 3-phase system can be expressed as shown in Eq. (9) with the concept of the d-q axis variables. Because the V_q with synchronous speed (ω) in the d-q coordinate method is equal to the magnitude of instantaneous voltage and V_d is zero, Eq. (10) can be obtained from Eq. (9).

$$P = \frac{3}{2} (V_d I_d - V_q I_q), \quad Q = \frac{3}{2} (V_q I_d + V_d I_q) \quad (9)$$

$$P = \frac{3}{2} |V_0| I_q, \quad Q = -\frac{3}{2} |V_0| I_d \quad (10)$$

Where, V_d, V_q are output voltages of d-axis and q-axis, I_d, I_q are output currents of d-axis and q-axis, and $|V_0|$ is

the magnitude of instantaneous voltage.

Therefore, It is clear that the instantaneous active power (P) is proportional to the magnitude of instantaneous voltage (V_0) and the current of q-axis (I_q) in same phase, and also that the instantaneous reactive power (Q) is proportional to the magnitude of instantaneous voltage (V_0) and the current of d-axis (I_d) with 90 degree phase difference.

3.2 Modified modeling of PV system

The conventional modeling of PV system as shown in ref. [7-8] can only deal with the small-scale active power of less than 60 [kW]. To overcome this problem, this paper adapts the Eq. (11) and Eq. (12) to compensate the process which converts DC voltage of the PI controller into 3-phase voltage. Specifically, V_d and V_q from the current control algorithm are transformed to 6 PWM signal in order to operate IGBT device and then 3-phase voltage is obtained by d-p coordinate method.

In other words, Eq. (11) and Eq. (12) which make each phase synchronize depending on magnitude variations of V_d and V_q , were introduced at current control algorithm and then these equations are compensated for the process of PI controller to control a desired current value of large scale active power.

$$\theta = \left(\tan^{-1} \frac{V_q}{V_d} \times \frac{180}{\pi} \right) \quad (11)$$

$$V_t = \left(\sqrt{V_q^2 + V_d^2} \right) \times \frac{\sqrt{3}}{\sqrt{2}} \quad (12)$$

Where, θ is desired phase angle of grid and V_t is desired voltage of distribution system.

3.3 Modified modeling based on the PSCAD/EMTDC

3.3.1 d-q transformation modeling

By using PSCAD / EMTDC, the d-q transformation modeling to convert 3-phase AC current into DC current is designed as shown in Fig. 6. Also, the inverse d-q transformation modeling to convert DC voltage into 3-phase AC voltage is implemented in Fig. 7.

3.3.2 Current control algorithm modeling

By using PSCAD/EMTDC, the detailed current control algorithm modeling by using Eq. (7) to Eq. (8) is designed as shown in Fig. 8.

And then, the reference currents (I_{qref} , I_{dref}) modeling to obtain the desired active power and reactive power based on the Eq. (10) is implemented as shown in Fig. 8.

3.3.3 Grid-connected inverter modeling

Fig. 10 is the modeling of grid-connected inverter to

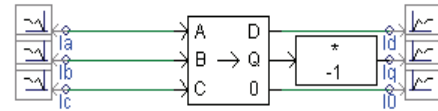


Fig. 6. Simulation of d-q transformation

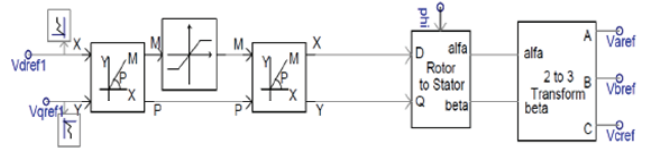


Fig. 7. Modeling of dq-abc transformation

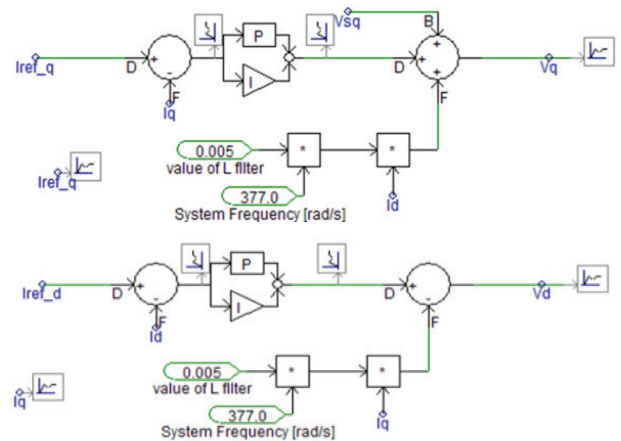


Fig. 8. Modeling of current control algorithm

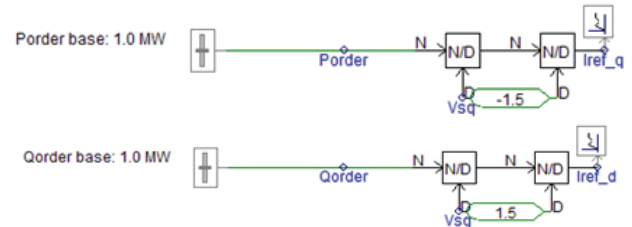


Fig. 9. Reference current modeling

convert DC voltage into 3 phase AC voltage using the IGBT devices and the modeling for sinusoidal PWM to produce the 3-phase AC sine waveform with 120° phase difference.

4. Modeling of SVR operation method

In order to determine optimal sending voltage, optimal setting values of LDC method should be calculated by the statistical analysis according to the relationship between ideal optimal sending voltages and total load currents as shown in Eq. (2). Based on the concept, the modeling of LDC method is implemented by PSCAD/EMTDC as shown in Fig. 11.

Using the tap changing concept of SVR in the Eq. (3), the tap control modeling with the bandwidth of 50% and time delay of 120 seconds is implemented as shown in Fig.

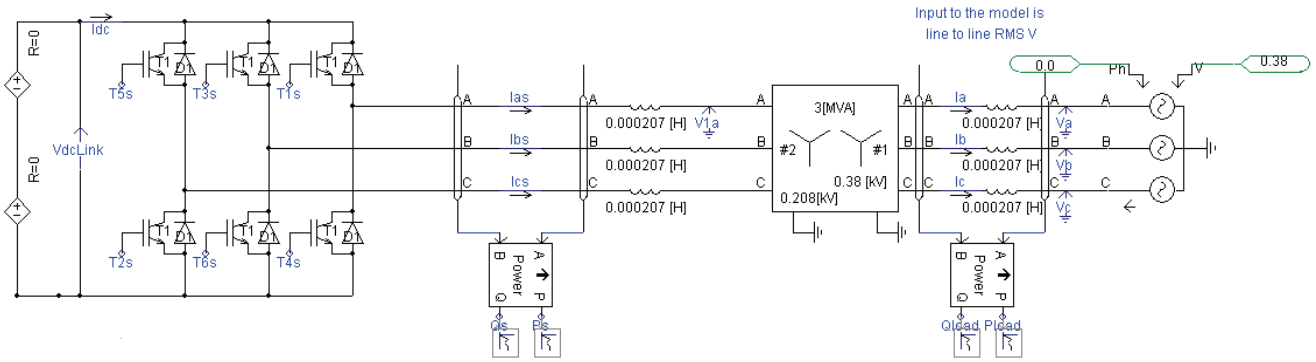


Fig. 10. Modeling for grid-connected inverter

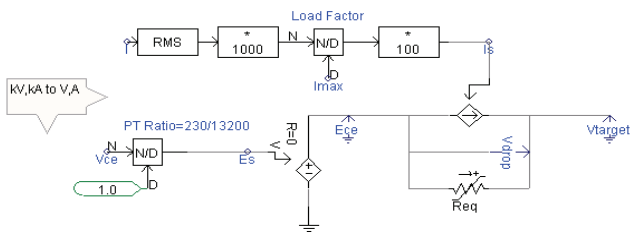


Fig. 11. Modeling of LDC method

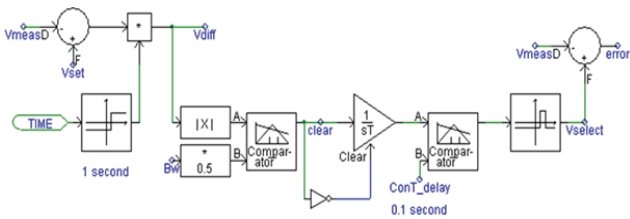
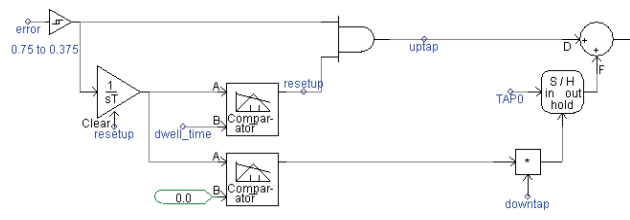
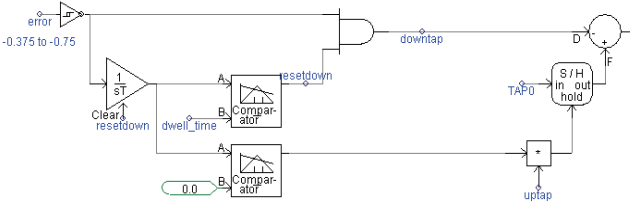


Fig. 12. Tap Control modeling



(a) Tap up modeling



(b) Tap down modeling

Fig. 13. Tap changing modeling

12, and also, the tap changing modeling is in Fig. 13. Where, Fig. 13 (a) is the modeling of tap up control and Fig. 13 (b) is the modeling of tap down control.

5. Case Studies

5.1 Verification of PSCAD/EMTDC modeling

To control the desired active power and reactive power of PV system, it is critical to obtain the value of reference current at the PSCAD/EMTDC modeling. Based on the Eq. (10), the relationship between reference current and active and reactive power can be expressed by Eq. (13).

$$I_{ref-q} = \frac{2}{3} \times \left[\frac{P}{V_q} \right], \quad I_{ref-d} = \frac{2}{3} \times \left[\frac{P}{V_d} \right] \quad (13)$$

Where, I_{ref-q} and I_{ref-d} are reference current of d-axis and q-axis, P and Q is desired active and reactive power, and V_d and V_q are output voltages of d-axis and q-axis. .

5.1.1 Characteristic of large-scale active power

To obtain large-scale active power of 1 [MW], the reference current (I_{ref-q}) can be calculated by Eq. (13), where the q-axis power system voltage of V_q is assumed as 0.310[kV].

$$I_{ref-q} = \frac{2}{3} \times \left[\frac{1}{0.310} \right] = 2.15$$

By performing the PSCAD/EMTDC simulation with the reference current, it is verified that the active power of 1 [MW] can be obtained as shown in Fig. 14.

5.1.2 Characteristic of large-scale reactive power

To control the large-scale reactive power of 1 [MVAR], the reference current (I_{ref-d}) can be obtained by Eq. (13), where the d-axis power system voltage of V_d is assumed as 0.102 [kV].

$$I_{ref-d} = \frac{2}{3} \times \left[\frac{1}{0.102} \right] = 6.54$$

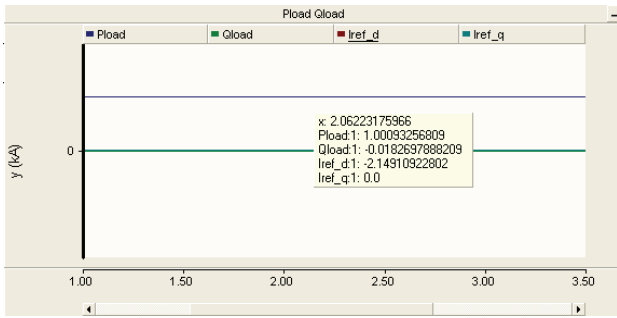


Fig. 14. Characteristic of 1MW active power

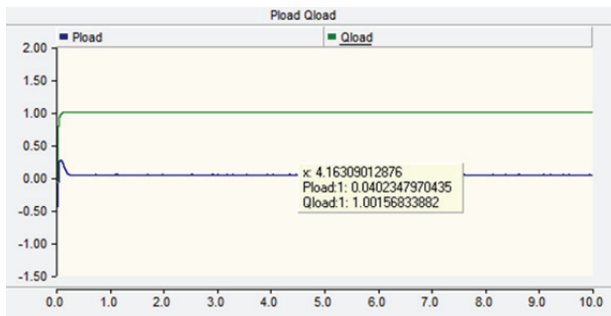


Fig. 15. Characteristic of 1MVAR reactive power

By performing the PSCAD/EMTDC simulation with the reference current, it is verified that the reactive power of 1 [MVAR] can be obtained as shown in Fig. 15.

5.2 Analysis of customer voltage variation

5.2.1 Simulation conditions

Based on the model distribution system of Fig. 1, distribution parameter and section data of primary feeder are assumed as Table 1 and Table 2, respectively. The turn ratio of pole transformer (P.tr) is considered as 13200V/230V and also voltage drops at the first and last customers of secondary feeder are considered as 2% and 8% of rated voltage (220V). Under these assumptions, the PSCAD/EMTDC modeling of distribution system

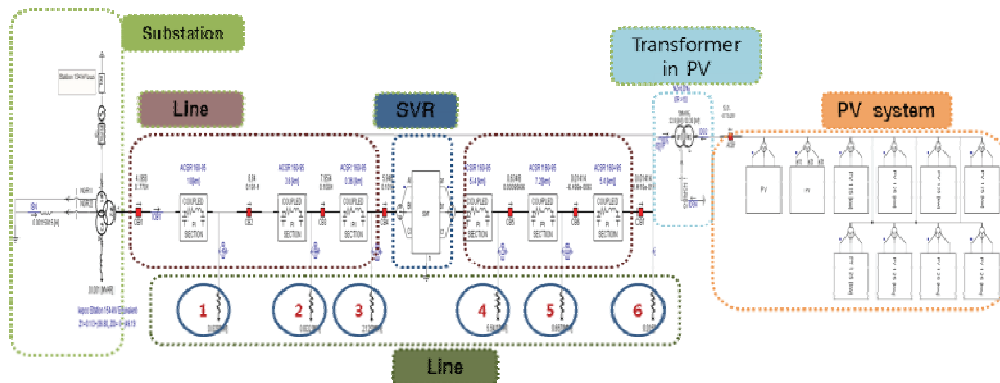


Fig. 16. Modeling of distribution system with PV system

Table 1. Distribution system parameter

% Impedance of Main Transformer	Z12(45MVA)	Z23(15MVA)	Z31(15MVA)	Base
	15.970	6.690	25.380	100MVA
Connection Type of M.tr	Y – Y – Delta			
Line to Line Voltage	22.9[kV]			
Power Factor	0.9			
Type of Load	Constant P (off-peak:1.5[MW], middle: 3[MW], peak:5[MW])			

Table 2. Section data of primary feeder

Feeder Number	Section Number	Impedance		Length (km)	P.tr Tap	Load ratio (%)	PV system (kW)
		R (Ω /km)	X (Ω /km)				
1	1	0.182	0.391	3.5	13200/230	8.3	0
	2	0.182	0.391	1.0	13200/230	8.3	0
	3	0.182	0.391	0.1	13200/230	21.3	0
	4	0.182	0.391	1.5	13200/230	55.4	0
	5	0.182	0.391	2.0	12600/230	6.6	0
	6	0.182	0.391	1.5	12600/230	0.2	3000
Total				9.6		100	3000

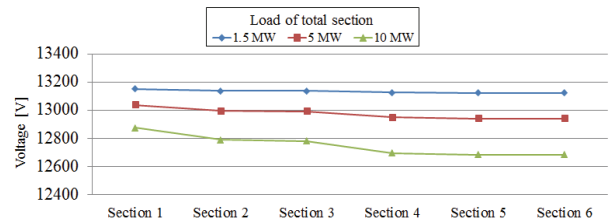


Fig. 17. Voltage variation of primary feeder without PV

interconnected with PV system can be expressed as shown in Fig. 16.

5.2.2 Characteristics of customer voltage variation

With the most severe conditions, it is assumed that off-peak load, middle load and peak load of one primary feeder (D/L) are 1.5 [MW], 5 [MW], and 10 [MW], respectively. Fig. 17 is the simulation results of primary voltage variation at each section based on the 13,200 [V] of phase voltage, when PV system is not interconnected.

Table 3. Customer voltage variation without PV

		Voltage [V] (Using 13,200[TAP])	
Load capacity of total section		The first customer point of P.tr	The last customer point of P.tr
1.5 MW	Section 1	219.85	218.68
	Section 2	219.62	218.26
	Section 3	219.59	218.23
	Section 4	219.12	217.56
	Section 5	227.99	226.01
	Section 6	227.99	226.01
5 MW	Section 1	217.87	214.02
	Section 2	217.15	212.79
	Section 3	216.98	212.45
	Section 4	216.25	209.98
	Section 5	223.29	218.89
	Section 6	223.29	218.89
10MW	Section 1	214.57	209.27
	Section 2	213.72	207.61
	Section 3	213.63	207.46
	Section 4	212.97	207.18
	Section 5	216.58	211.78
	Section 6	216.58	211.78

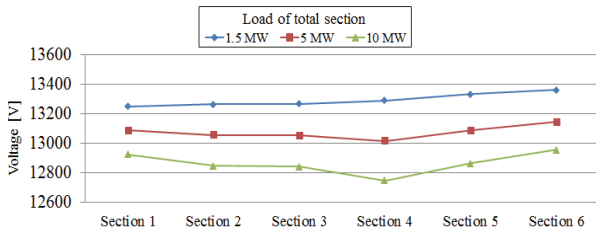


Fig. 18. Voltage variation of primary feeder with PV system of 3 [MW]

Table 3 is the customer voltage characteristic of secondary feeder from section 1 to 6, which is calculated from the Fig. 16. During the off-peak load of 1.5 [MW], it is clear that the voltage variation of customers is very small and reasonable characteristics. And also, in the peak load of 10 [MW], the customer voltages have reasonable conditions. Therefore, when the PV system is not interconnected with distribution system, it is confirmed that all of customer voltages of each section can be maintained within the allowable limits ($220[V] \pm 6\%$).

However, Fig. 18 is the voltage variation characteristics of primary feeder at each section when PV system of 3 [MW] is located at section 6. Compared to the Fig. 17, it is clear that the overvoltage phenomena at all of sections in primary feeder are occurred by the reverse power flow of PV system. And also, the overvoltage characteristic at the off-peak load of 1.5 [MW] is much bigger than the peak load of 10 [MW], because the reverse power flow of PV system at off-peak load can influence the bigger impact to distribution system than the peak load.

From the Fig. 18, the customer voltage characteristic of secondary feeder from section 1 to 6 is obtained as shown in Table 4. It is clear that some customer voltages of section 6 at the off-peak load cannot be maintained within

Table 4. Customer voltage variation with PV system of 3 [MW]

		Voltage [V] (Using 13,200[TAP])	
Load capacity of total section		First customer point of P.tr	Last customer point of P.tr
1.5MW	Section 1	221.17	222.34
	Section 2	221.43	222.87
	Section 3	221.47	222.95
	Section 4	221.97	223.95
	Section 5	232.61	231.29
	Section 6	233.15	231.83
5MW	Section 1	218.45	216.92
	Section 2	218.27	216.55
	Section 3	218.25	216.51
	Section 4	218.28	216.58
	Section 5	225.82	221.42
	Section 6	226.80	222.40
10MW	Section 1	217.02	211.87
	Section 2	216.85	209.48
	Section 3	216.11	208.92
	Section 4	215.83	208.32
	Section 5	223.88	217.48
	Section 6	224.61	218.91

Table 5. Customer voltage conditions with SVR

		Voltage [V] (Fixed method)		Voltage [V] (LDC method)	
Load capacity of total section		First customer point	Last customer point	First customer point	Last customer point
1.5 MW	Section 1	221.17	222.34	219.17	220.34
	Section 2	221.43	222.87	218.95	220.77
	Section 3	221.47	222.95	218.37	220.65
	Section 4	221.97	223.95	217.77	220.67
	Section 5	232.61	231.29	230.11	229.09
	Section 6	233.15	231.83	231.97	229.67
5 MW	Section 1	218.45	216.92	216.45	214.82
	Section 2	218.27	216.55	216.77	214.65
	Section 3	218.25	216.51	216.25	214.39
	Section 4	218.28	216.58	216.18	213.42
	Section 5	225.82	221.42	223.22	219.22
	Section 6	226.80	222.40	224.17	220.42
10 MW	Section 1	217.02	211.87	215.02	209.73
	Section 2	216.85	209.48	214.85	207.58
	Section 3	216.11	208.92	214.09	206.78
	Section 4	215.83	208.32	213.53	206.23
	Section 5	223.88	217.48	221.82	215.47
	Section 6	224.61	218.91	222.35	216.79

allowable limits with the overvoltage phenomena by the reverse power flow of PV system. Therefore, it is clearly expected that severe voltage quality problems may be occurred if the large-scale PV system is located at the end section of primary feeder.

5.2.3 Voltage compensation with SVR

In order to improve voltage quality problem like overvoltage phenomena from the installation of PV systems as mentioned earlier, this paper adopts that SVR to control the primary feeder is installed at the section 3.

Among the various operation method of SVR, this paper shows the comparison result between fixed method and LDC method as shown in Table 5. Where, the fixed method is widely used in power utility in Korea, which is operated by fixed sending voltage of 13200[V] based on the phase voltage. It could have possibility of customer voltage problems for the rapid voltage variation. To overcome these problems, this paper presents LDC method which can control the sending voltage of SVR depending on the load variation. Compared to Table 4 without SVR, it is clear that all of customer voltages can be maintained within the allowable limits according to the voltage control method (LDC method) of SVR. Therefore, it is confirmed that the operation of SVR can make the customer voltage of distribution system with PV system keep better voltage conditions.

6. Conclusions

This paper has proposed the modified modeling of PV system based on the PSCAD/EMTDC and optimal control method of customer voltages in real distribution system interconnected with the PV systems. The main results are summarized as follows.

- (1) It is confirmed that the overvoltage phenomena in primary feeder is occurred by the reverse power flow of PV system. And also, the overvoltage phenomena at the off-peak load is much bigger than the peak load, because the reverse power flow of PV system at off-peak load can influence the bigger impact to distribution system than the peak load.
- (2) When the PV system is interconnected with distribution system, some customer voltages cannot be maintained within allowable limits ($220[V] \pm 6\%$). Therefore, it is clear that severe voltage quality problems may be occurred if the large-scale PV system is located at the end section of primary feeder.
- (3) With the optimal control method of SVR, it is clear that all of customer voltages can be maintained within the allowable limits compared to customer voltages without SVR. Therefore, it is confirmed that the operation of SVR can be practical tool for the better voltage conditions in distribution system interconnected with PV system.

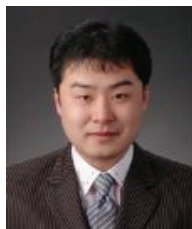
Acknowledgements

This work was supported by the Power Generation & Electricity Delivery Core Technology Program of the Korea Institute of Energy Technology Evaluation and Planning (KETEP) granted financial resource from the Ministry of Trade, Industry & Energy, Republic of Korea (No. 20131020400720)

References

- [1] IEEE 1547.6 "IEEE Standard conformance Test Procedures for Equipment Interconnecting Distributed Resources with Electric Power System", June, (2009)
- [2] IEEE 1547.1 "IEEE Standard conformance Test Procedures for Equipment Interconnecting Distributed Resources with Electric Power System", June, (2005)
- [3] IEEE 1547 "IEEE Standard for Interconnecting Distributed Resources with Electric Power System", July, (2003)
- [4] D. Rho and Hasegawa, J, "A study on the optimal voltage regulation methods in power distribution systems interconnected with dispersed energy storage and generation systems", JIEE, Vol. 8, No. 4, pp. 702~707, 1995
- [5] B. Kim and D. Rho, "Optimal Voltage Regulation Method for Distribution System with Distributed Generation Systems Using the Artificial Neural Networks", JEET 2013, Vol. 8, No. 4, pp. 712~718, 2013
- [6] B. Kim and D. Rho, "Implementation of Monitoring and Control Systems for 50KW PV Systems Using the Wire-Wireless Network", GDC 2011, CCIS 261, pp. 45-53
- [7] Abdulrahman Kalbat. "PSCAD Simulation of Grid-Tied Photovoltaic Systems and Total Harmonic Distortion Analysis", IEEE EPECS 2013 3rd International Conference on, 2013.10.
- [8] Naoyuki Aizawa, Hisao Kubota, "Analysis of common-mode voltage elimination of PWM inverter with auxiliary inverter", IEEE-ICEMS 2010 International Conference on, pp889-893, 2010.10
- [9] D. Rho and M. Kim, "A study on the Optimal Operation of Line Voltage Regulator (SVR) in Distribution Feeders", 2004 IFAC Symposium, Seoul, South Korea, 2004. 9.
- [10] M. Kim, D. Rho, J. Kim, K. Kim, "Optimal Operation Method of Multiple Voltage Regulators in Distribution Systems Interconnected with Dispersed Storage and Generation Systems", Trans. KIEE. Vol. 54A. No. 2, 2005. 2.
- [11] Sohee Kim and Daeseok Rho, "Development of Evaluation Systems for Bi-Directional Protection Coordination in Distribution System Considering Distributed Generations", IJGDC 2012, Vol. 5, No. 1, pp. 23-32. 2012
- [12] D. Rho, K. Kook and Y. Wang, "Optimal Algorithms for Voltage Management in Distribution Systems Interconnected with New Dispersed Sources", JEET 2011, Vol. 6, No. 2, pp. 192~201, 2011
- [13] H. Soi, H. Yakabe, H. Kakimoto, T. Hayashi & M. Kanori, "Development of High Voltage Distribution Line Management System", IEEEJP & Society, No. 32 (2006)
- [14] Daeseok Rho and Byeongi Kim, "Optimal Voltage

Regulation Method for Distribution Systems with Distributed Generation Systems Using the Artificial Neural Networks”, JEET, Vol. 8, No. 5, 2013



Byung-Ki Kim He received the B.S. degree and M.S. degree in Electrical Engineering from Korea University of Technology and Education, Cheon-An, South Korea, in 2008 and 2012. And he is currently pursuing the Ph.D. degree at KOREATECH, Cheon-An, South Korea. He is interested in renewable energy resources and new power distribution systems.



Sung-sik Choi He received B.S degree in information and communication engineering from Korea University of Technology and education. And he is currently pursuing the M.S degree at KOREATECH, Cheon-An, South Korea. He is interested in renewable energy resources.



Yong-Peel Wang He received the B.S., M.E. and Ph. D degree in Electrical Engineering from Dong-A University, Busan, South Korea, in 1992, 1994 and 1998, respectively. He was a post-doctoral fellow from 1999-2001 at Canterbury University, New Zealand and a lecturer from 2001-2008 at Dong-

A university. He has been working as a Senior Re-Searcher at Electrical Industry Research Institute of Korea since 2009. His research interests include operation of power distribution systems, HVDC power systems, electromagnetic transient, and power quality.



Eung-Sang Kim He received the B.S. degree from Seoul Industrial University, Korea, in 1988 and the M.S. and Ph.D. degrees in Electrical Engineering from Soongsil University, Korea, in 1991 and 1997, respectively. Since 1991, he has been with the Department of Power Distribution System at the

Korea Electric Research Institute (KERI), Korea, where he is currently a Principal Researcher and serves as a member of Smart Grid Project Planning committee in Korea. His interests are new and renewable energy system designs and developments of wind power, photovoltaic and fuel cell energy conversion systems.



Dae-Seok Rho He received the B.S. degree and M.S. degree in Electrical Engineering from Korea University, Seoul, South Korea, in 1985 and 1987, respectively. He earned a Ph.D. degree in Electrical Engineering from Hokkaido University, Sapporo, Japan in 1997. He has been working as a pro-

fessor at Korea University of Technology and Education since 1999. His research interests include operation of power distribution systems, dispersed storage and generation systems and power quality.